Analysis of Load, Temperature, and Shrinkage Effect on Continuously Reinforced Concrete Pavement

James Ma and B. Frank McCullough, Center for Highway Research, University of Texas, Austin

A computer program—CRCP-2—for the analysis of load, temperature, and shrinkage effects on a continuously reinforced concrete pavement is presented. The transverse cracking of continuous pavements is the result of the restraint of the pavement slab to dimensional changes induced by internal and external forces. The formation of transverse cracks can be attributed to two distinct and basic mechanisms: (a) the internal forces associated with decrease in temperature and drying shrinkage and (b) the externally induced stress caused by wheel loads. The CRCP-2 computer program combines the stress caused by internal forces and the flexural stress under wheel load. The internal stress is determined by using the one-dimensional axial structural model that simulates the mechanistic behavior of the composite slab. The wheel-load stress can be determined either externally by slab-analysis methods or internally within the program by using the Westergaard equation for interior loading and inputting the magnitude of the wheel load, the wheel-base radius, and the modulus of subgrade. A series of problems is solved by using the CRCP-2 computer program. The results show that external load, when combined with internal forces, induces more cracks to develop and that both steel stress and crack width decrease as crack spacing decreases. The function of steel reinforcement in continuously reinforced concrete pavement is to control crack spacing; higher steel percentage means higher restraint to the concrete, which causes more cracks to develop. The function of the slab thickness is to resist the tensile stress under wheel load; thicker slab usually means wider crack spacing. It is concluded that the inclusion of both wheel load and internal forces makes it possible to predict more realistically and more accurately the actual crack spacing, the crack width, and the steel stress in the pavement system and the slab thickness and the steel percentage must be properly designed to (a) withstand the internal forces developed from restrained-pavement volume changes, (b) keep cracks tightly closed, and (c) avoid excessive cracking. Over-design of slab thickness means that a larger volume of concrete will undergo thermal contraction and drying shrinkage, which causes the internal force in the continuous pavement to increase, although an increase in slab thickness will reduce the tensile stress on the bottom fiber of the slab under wheel load. Over-design of steel reinforcement will cause excessive cracking and thus lose the integrity of the pavement to act as a continuous slab, although a higher steel percentage will reduce the crack width and prevent the passage of water from the surface of the pavement to the subgrade.

The changes in dimension in a continuously reinforced concrete pavement that are caused by drying shrinkage of the concrete and by temperature variation after curing have been investigated and a design method—CRCP-1—was developed in 1975 (1). The theoretical model is based on the material properties; the stress; the strain interactions among steel, concrete, and subgrade; and the internal forces caused by a temperature decrease and shrinkage of the slab.

Figures 1 and 2 show the geometric model used to develop the basic equations for the CRCP-1 design method. Because of the accumulated friction and the terminal treatments used in the construction, the slab model assumes an anchorage at each end and the pavement within the anchorages will maintain a fixed length.

The difference between the thermal coefficients of steel and concrete, together with the drying shrinkage of concrete, enables us to determine the internal stress in the reinforced slab. By using the friction-movement characteristics of the slab and the soil, the degree of restraint of the supporting medium can be estimated. By establishing the equilibrium in the system, the stress of one material can be correlated with the stress of the adjacent materials. Finally, the crack spacing is determined by comparing the concrete stress with the concrete strength at each time interval.

In the development of the model, the following assumptions were made:

1. A crack occurs when the concrete stress exceeds the concrete strength and, after cracking, the concrete stress at the location of the crack is zero.
2. The concrete and steel properties are linearly elastic.

Figure 1. Full length of continuously reinforced concrete pavement.

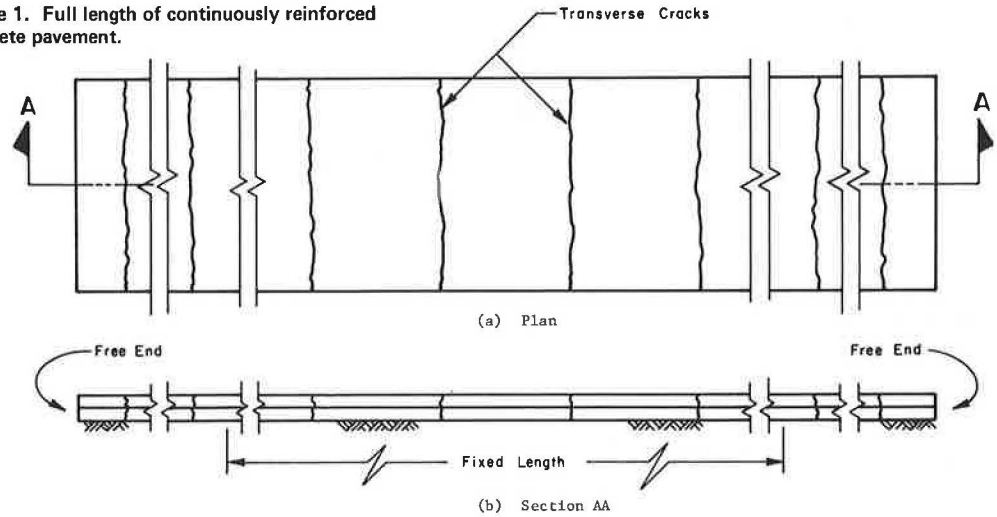

3. In the fully bonded sections of the concrete slab, there is no relative movement between the steel and the concrete.
4. The force displacement curve that characterizes the frictional resistance between the concrete slab and the underlying base is elastic.
5. Temperature variations and shrinkage caused by drying are uniformly distributed throughout the slab and, hence, a one-dimensional axial structural model is adopted for the analysis of the problem.
6. Material properties are independent of space.
7. The effects of creep of concrete and slab warping are neglected.

PRIMARY CONCEPTS

The mechanistic behavior of the CRCP model is summarized briefly below.

Steel and Concrete Interaction

In a fully bonded section of a continuously reinforced concrete pavement, the total change in length in the concrete will be the same as the change in the length of the steel. Thus, the difference in the thermal coefficients of expansion and contraction of the steel and of the concrete plus the drying shrinkage of the concrete result in a steel-and-concrete strain history that can be modeled by a mathematical relationship. By converting strains into stresses based on their individual moduli of elasticity, the stress history of the concrete can be written as the function of the stress history of the steel.

Steel Boundary Conditions

The total length of the pavement within the fictitious anchorages is fixed, which implies that the integral of the steel strains along the slab (the sum of the area under the steel-strain diagram) will equal the pavement shortening. The steel stress at any point can be written as a function of the steel stress at any other point along the slab.

Equilibrium

Figures 3 and 4 show a free-body diagram for the CRCP model. By summing all the forces, the steel and the concrete stresses between the cracks will be balanced by the sum of the steel stresses at the crack and the frictional resistance between the slab and the base.

By converting the concrete stresses between the cracks into functions of steel stress, the steel stress (and then the concrete stress and the slab movement) can be readily calculated, provided that the frictional resistance is known. The frictional resistance, however, is not a constant force because it depends on the magnitude of the movement of the slab; the larger the movement, the larger the resulting frictional force. The movement of the slab is its length times the total strain and the stress of the concrete and steel must be determined to find the strain; thus, an interactive process that involves the following steps (see Figure 5) is needed to determine the frictional forces and the stresses in the slab:

1. Assume zero friction and solve for the strain of the concrete along the slab.
2. Sum the strains and solve for the movement of the slab (Y_1).

Figure 2. Geometric model of continuously reinforced concrete pavement.

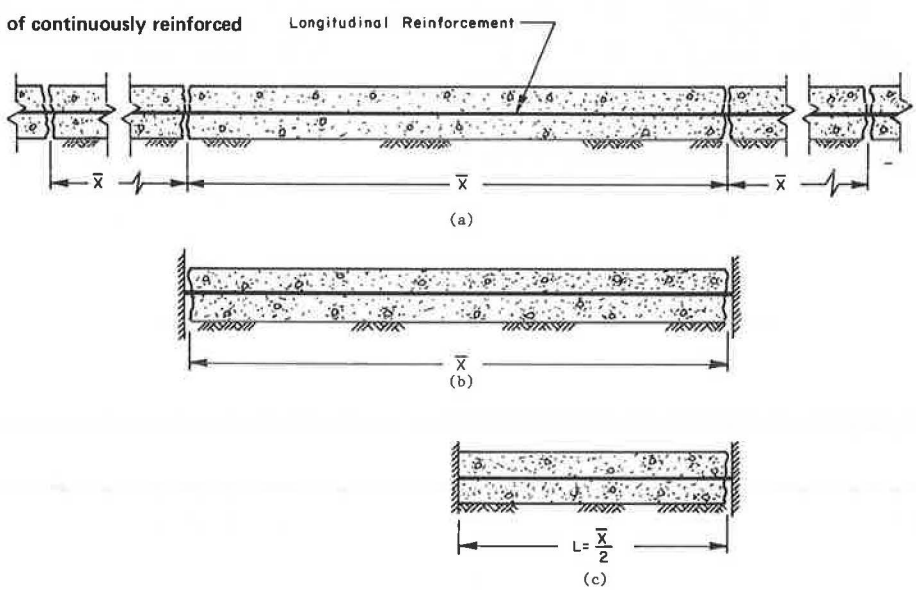

Figure 3. Forces in CRCP free-body diagram.

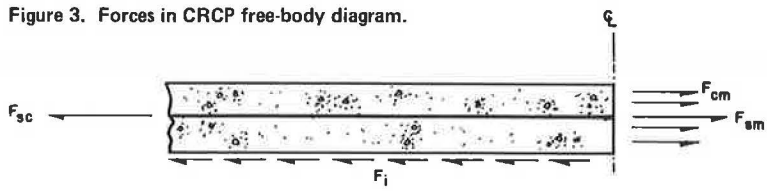

3. Use a friction-movement (F-M) curve, obtained through laboratory experiments, to locate the frictional force (F_2) that corresponds to the movement found in step 2.
4. Reenter F_2 from step 3 into the basic equations and solve for the movement (Y_2).
5. Reenter Y_2 into the F-M curve and solve for F_3.
6. Use the average of F_2 and F_3 (F_4) to solve for the compressive movement (Y_{4c}) by using the basic equations and the expansive movement (Y_{4e}) by using the F-M curve [if $Y_{4c} > Y_{4e}$, $F_5 = (F_2 + F_4)/2$, and if $Y_{4c} < Y_{4e}$, $F_5 = (F_3 + F_4)/2$].
7. Return to step 6 and use the new frictional force until the movement obtained by using the equations falls within the tolerance range of the movement obtained by using the F-M curve.
8. Use the final frictional force to solve for the steel stress at the crack and the concrete stress at the middle of the slab.

INCLUSION OF WHEEL-LOAD STRESS

When a crack occurs, the tension that was carried by the concrete will be taken up by the steel. The concrete stress will, therefore, be zero at the crack and increase to its maximum in tension at the middle of the slab. This high tension stress at the middle of the slab is the result of the accumulated frictional resistance of the base plus the restraint on contraction of the concrete by the steel.

If the effect of warping caused by the temperature variance is neglected, the tensile stress caused by the internal forces will be uniformly distributed across the depth of the slab (see Figure 6b). Theoretically, the maximum value of this tensile stress will be near the midpoint between a pair of cracks where the highest frictional resistance is accumulated. The stress caused by external forces, on the other hand, will be in compression on the top fiber and in tension on the bottom fiber (Figure 6c). The maximum value of the combined stresses will then be at the bottom fiber of the slab at the midpoint between two cracks. Figure 6d shows the

Figure 4. Free-body diagram of element in CRCP model.

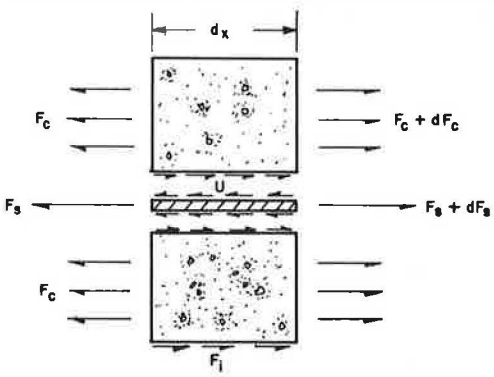

Figure 6. Stresses at center of concrete slab caused by wheel loads and volume changes.

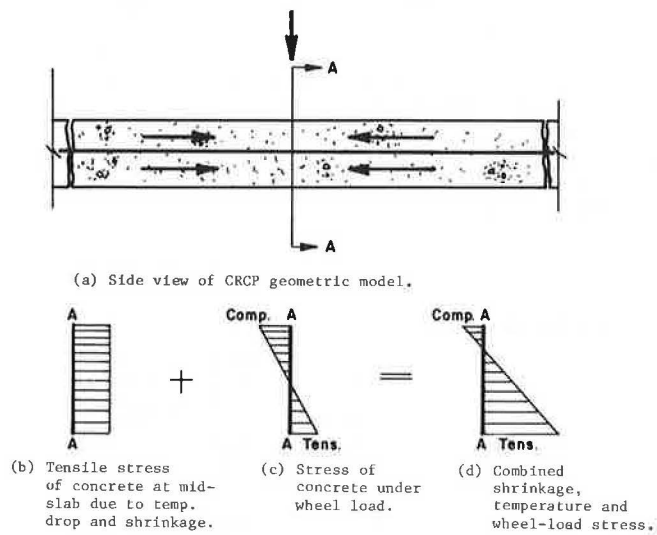

Figure 5. Binary search technique as applied to frictional resistance-movement curve.

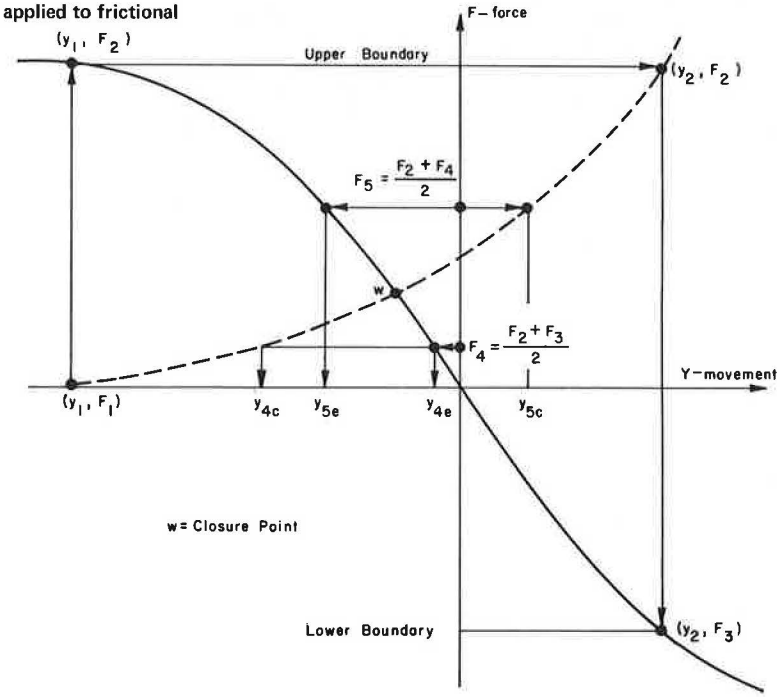

stress diagram for a wheel-load stress superimposed by a tensile stress at the middle of the slab caused by drying shrinkage and temperature decrease, in which

$$\sigma_{TOT} = \sigma_{INT} + \sigma_{EXT} \quad (1)$$

where

σ_{TOT} = combined external and internal stresses,
σ_{INT} = tensile stress caused by drying shrinkage and temperature decrease, and
σ_{EXT} = tensile stress at bottom fiber of the slab under wheel load.

New cracks will form when σ_{TOT} exceeds the tensile strength of the concrete. After these cracks have developed, the external load will be moved to a new position, the midpoint between the newly developed crack and an adjacent crack. This process continues until equilibrium is established.

The inclusion of wheel-load stress led to the development of the CRCP-2 computer program, which is briefly summarized in the flow diagram shown in Figure 7.

The tensile stress caused by the external load is solved in the CRCP-2 computer program by using Westergaard's equation for interior loading. The user may choose, however, to solve the wheel-load stress by some other method. The program allows the option of using either the wheel-load mass or the wheel-load stress as input.

STRESS IN SLAB CAUSED BY WHEEL LOADS

The steel reinforcement in continuous pavements is not designed to carry the tensile stress at the bottom when wheel loads are applied. In fact, most steel bars in rigid pavements are placed at the middepth of the slab (i.e., the neutral surface) so that cracks will be kept tightly closed and the time for water to seep through will be greater than the surface runoff time (which prevents passage of water from the surface to the subgrade). When the steel bars are placed at the neutral surface, the compression on the top fiber and the tension on the bottom fiber of a reinforced slab will be the same as for a nonreinforced slab. Several methods available for the analysis of a concrete slab under wheel loads are discussed below.

Westergaard Interior Equation

The Westergaard equation for interior loading can be used to predict the tensile stress at the bottom fiber of a slab (2). The resistance to deformation of the slab under a wheel load depends on the relative stiffness of the supporting media and the slab; the stiffer the slab and the weaker the subgrade, the greater the stress. Westergaard defined the relative properties of these two materials as the radius of relative stiffness (ℓ)

$$\ell = [E_c D^3/12(1 - \mu^2)k]^{1/4} \quad (2)$$

Figure 7. Flow diagram for CRCP-2.

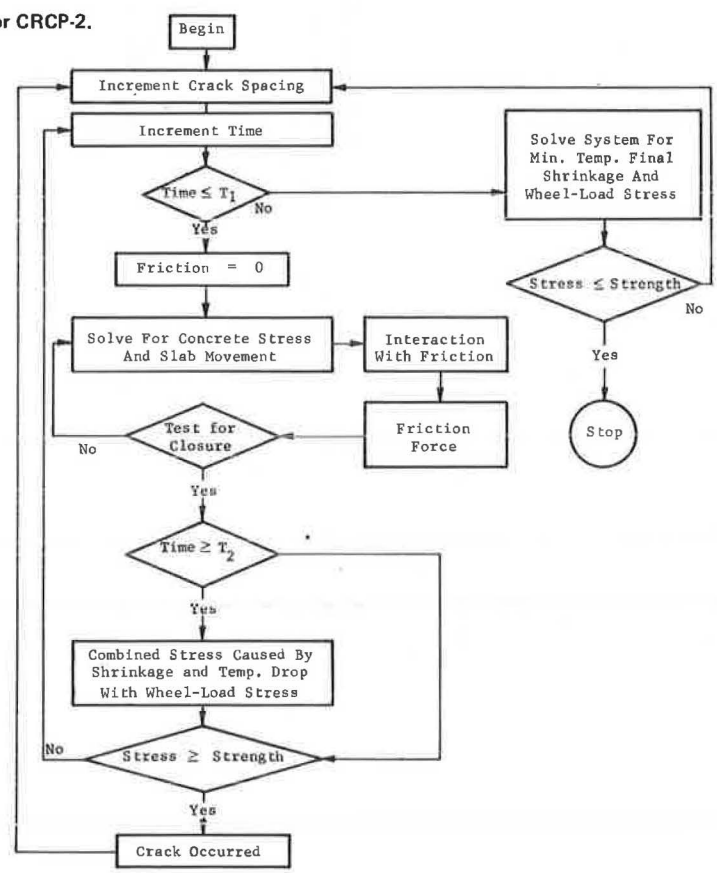

T_1 = Time for concrete to gain full strength.
T_2 = Time when wheel load is applied.

where

E_c = modulus of elasticity of concrete slab (kPa or lbf/in^2),
D = thickness of slab (m or in),
μ = Poisson's ratio, and
k = modulus of subgrade reaction (kN/m or lbf/in^3)

and the tensile stress at the bottom of the slab for interior loading (σ_i)

$$\sigma_i = (0.3162\ P/D^2)\ (\log D^3 - 4\log a - \log k + 6.478) \quad (3)$$

where

a = radius of tire contact area (m or in) and
P = applied load (kN or lbf).

(The coefficients in Equations 3-5 apply to U.S. customary units only; therefore, values in Figures 8-15 are not given in SI units.)

If it is assumed that a planar cross section remains planar and perpendicular to the neutral surface during loading, the theory of elasticity leads to the conclusion that the peak moment and, thus, the peak tensile stress at the bottom of the slab are infinite. However, if the effects of the deformation caused by local stress in the immediate neighborhood of a concentrated load are included, this assumption cannot be made and the tensile stress at the bottom fiber of the slab will be rounded off. A calculation made by using Nadai's analysis (3) shows that the stress can be found by using the special theory that considers local stress at the point of loading if a is replaced by an equivalent radius (b) in which

$$b = (1.6a^2 + D^2)^{1/2} - 0.675D \qquad (a \leq 1.724D) \quad (4)$$

and

$$b = a \qquad (a \geq 1.724D)$$

The tensile stress at the bottom for interior loading when a < 1.724D becomes

$$\sigma_i = (0.3162\ P/D^2)\{\log D^3 - 4\log[(1.6a^2 + D^2)^{1/2} - 0.675D] - \log k + 6.478\} \quad (5)$$

Discrete Element

Several computer programs have been developed to determine the wheel-load stress of the slab. The discrete-element method developed by Hudson and Matlock (4, 5) is a powerful analytical tool based on the biharmonic equation (6), which states that the fourth-order differential of the deflection multiplied by the stiffness is equal to the applied load. This fourth-order differential is solved for by the central-differential approximation in which the differential of the deflection is the change of deflection between adjacent stations divided by the distance between those stations. The stiffness of the system is obtained by replacing the slab by x-bars and y-bars to simulate bending stiffness, by torsional bars to simulate torsional stiffnesses, and by elastic joints to connect the whole system together. Because of the large number of simultaneous equations that relate the relative forces that act on each element, a direct matrix manipulation technique (7) is used to obtain the deflection at each joint.

Two approaches are recommended for the computation of the wheel-load stress. The first is to determine the wheel-load stress internally by using Westergaard's equation for interior loading, for which the user needs only to input the magnitude of the wheel load, the wheel-base radius, and the modulus of subgrade. Westergaard's equation was selected for three reasons: (a) it is easy to apply and the solution obtained is the tensile stress directly under the wheel load, (b) the computational time required is minimal, and (c) it is the most reliable closed-form solution available. From laboratory tests on concrete slabs, it was concluded that the values derived by using Westergaard's theoretical formula correlate closely with the experimental values (8, 9).

The second approach is to determine the wheel-load stress externally and input the maximum concrete tensile stress obtained into the CRCP-2 program. For edge loads, the tensile stress can be obtained by using Westergaard's equation for edge loadings. For pavements that have nonuniform slab thicknesses or nonuniform soil supports, the tensile stress under a wheel load can be determined by the discrete-element method. This open-form solution allows us to consider voids underneath the pavement, and cracks can be modeled by reducing the bending stiffness along the crack (10). However, the use of this method requires the investigation of the load transfer between cracks, which includes (a) aggregate interlock, (b) shear resistance by steel reinforcement, and (c) moment transfer if the crack width is small enough for the slab on each side to make contact, and concepts for modeling these effects are still being developed.

Neither of these approaches considers the fatigue of the concrete slab caused by repetitive loadings. A

Figure 8. A-series: crack spacing under wheel-load stresses applied on 28th day versus time.

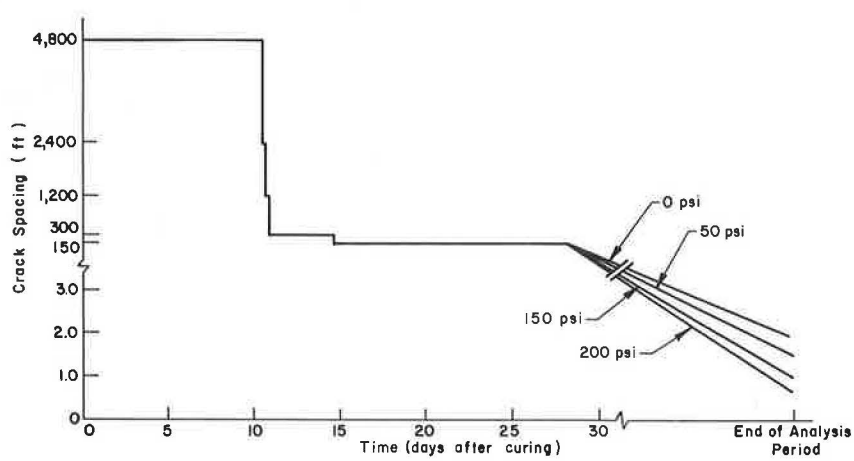

safety factor is needed in these approaches when they are used for design.

EFFECT OF EXTERNAL LOAD

Five series of problems were solved by using the CRCP-2 program. The A-series was developed to study the effect of wheel-load stress on the crack spacings of continuously reinforced concrete pavement. In the B-series, the effects of wheel-load stress on crack width, crack spacing, and steel and concrete stress were examined. In the C-series, the steel percentages are varied and the effects on crack spacing, crack width, and steel and the concrete stresses (with and without wheel-load stress) examined. The D-series shows the effects of wheel loads applied on slabs that have different thicknesses. The E-series shows the effect of wheel load applied at various ages after the placement of the slab. The fixed and variable input parameters for the A-series are given below [1 cm = 0.4 in, 1 MPa = 145 lbf/in^2, (μm/m)/°C = 1.8(0.000 001 in/in)/°F, 1 kN/m^3 = 6.37 lbf/ft^3, and t°C = (t°F - 32)/1.8], and the results are shown in Figure 8.

Fixed Parameter	Value
Steel property	
P, %	1.0
Diameter, cm	1.25
Yield stress, MPa	41.3
Modulus, GPa	20.0
Coefficient of thermal expansion, (μm/m)/°C	9.0
Concrete property	
D, cm	25.4
Coefficient of thermal expansion, (μm/m)/°C	9.0
Shrinkage coefficient, %	0.04
Unit mass, kN/m^3	13.6
Compression strength, MPa	4.1
Temperature data, °C	
Curing	24
Daily min	
1-10	18
11-16	10
17-28	10
Min	4.5
Cold time, d	90
Friction	
Pressure, kPa	6.9
Movement, cm	-0.25

Variable Parameter	Problem 1	2	3	4
External load				
Wheel-load stress, MPa	0	34.5	103.5	138
Time applied, d	-	28	28	28

Four different loads were used, all applied on the 28th day. The addition of the bending stress caused by the external load to the existing internal force caused by the restrained-pavement volume changes leads to a higher tensile stress and causes new cracks to form. Thus, the final crack spacing decreases as the magnitude of the external load increases, and this decrease will cause other variables to change also, as is illustrated in the following problem series.

The fixed and variable input parameters for the B-series are given below.

Fixed Parameter	Value
Steel property	
P, %	0.5
Diameter, cm	1.52
Yield stress, MPa	41.3
Modulus, GPa	20.0
Coefficient of thermal expansion, (μm/m)/°C	9.0
Concrete property	
D, cm	25.4
Coefficient of thermal expansion, (μm/m)/°C	9.0
Shrinkage coefficient, %	0.04
Unit mass, kN/m^3	13.6
Compression strength, MPa	4.1
Temperature data, °C	
Curing	24
Daily min	
1-10	10
11-16	10
17-28	10
Min	4.5
Cold time, d	90
Friction	
Pressure, kPa	6.9
Movement, cm	-0.25
External load	
Time applied, d	28

Figure 9. B-series: crack spacing, crack width, steel stress, and maximum concrete stress at end of analysis period versus external load.

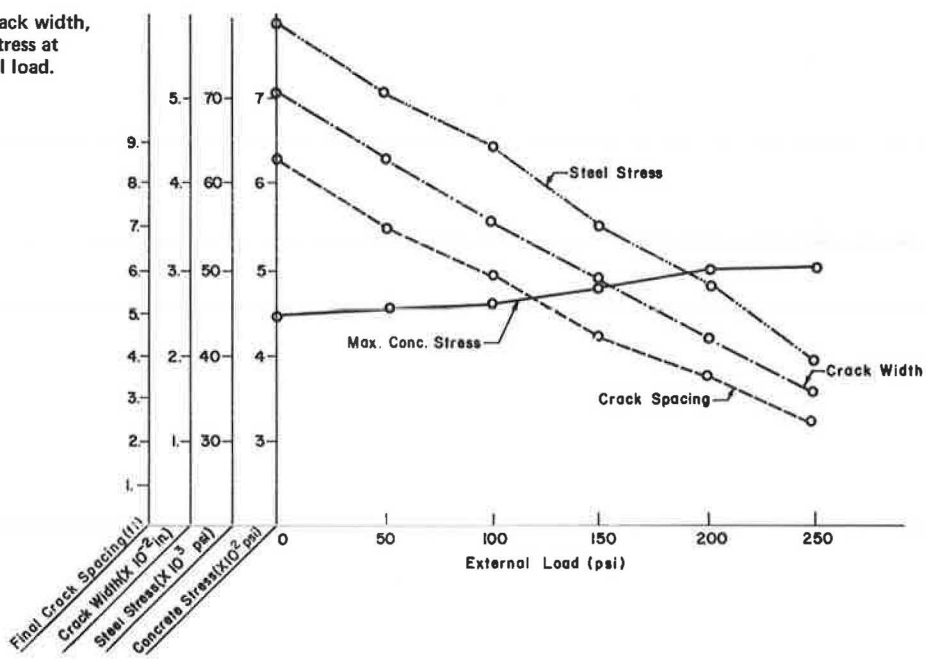

Variable Parameter	Problem 1	2	3	4	5	6
External load						
Wheel-load stress, MPa	0	34.5	69.0	103.5	138.0	172.5

Figure 9 is a composite that shows the effects of wheel-load stress on the behavior of the various variables. Thus, the final crack spacing decreases when heavier external loads are applied, and this reduction in crack spacing decreases the frictional resistance between the slab and the subgrade because the contact area is reduced. Subsequently, the crack width and the forces transmitted to the steel from the reduced restraint also decrease. The final concrete stress is a more or less straight line for different magnitudes of external loads. This phenomenon will be discussed below.

The results of this problem series show that the addition of external load reduces both the steel stress and the crack width in continuously reinforced concrete pavements by forcing more cracks to develop. The reduction of these two variables can be favorable for the design as long as the crack spacing is maintained at an acceptable level.

The fixed and variable input parameters for the C-series are given below (1kN = 2.25 lbf).

Fixed Parameter	Value
Steel property	
Diameter, cm	1.25
Yield stress, MPa	41.3
Modulus, GPa	20.0
Coefficient of thermal expansion, (μm/m)/°C	9.0
Concrete property	
D, cm	25.4
Coefficient of thermal expansion, (μm/m)/°C	9.0
Shrinkage coefficient, %	0.04
Unit mass, kN/m³	13.6
Compression strength, MPa	4.1
Temperature data, °C	
Curing	24
Daily min	
1-10	10
11-16	10
17-28	10
Min	4.5
Cold time, d	90
Friction	
Pressure, kPa	6.9
Movement, cm	-0.25
External load	
Time applied, d	28

Variable Parameter	Problem 1	2	3	4	5	6	7	8
Steel property								
P, %	0.5	0.7	0.9	1.2	0.5	0.7	0.9	1.2
External load								
Wheel load, kN	0	0	0	0	-	-	-	-
Wheel-load stress, MPa	0	0	0	0	69.0	69.0	69.0	69.0

The steel reinforcement in a continuously reinforced concrete pavement does not prevent cracking. On the contrary, it induces cracks because the volume change in the concrete is restrained by the steel bars and because of the subgrade friction. However, steel in the slab also keeps the cracks tightly closed. As shown in Figure 10, an increase in the steel percentage in the slab is associated with a decrease in crack spacing and with even smaller crack spacing when an external load is applied. The reduction of crack spacing in turn causes the crack width and the steel stress to decrease, as shown in Figures 11 and 12.

The final concrete stresses plotted in Figure 13 do not show a trend. Increasing the steel percentage causes the concrete stress to increase and then to decrease. The difference in concrete stress between the slab that had a wheel load applied to it and the slab that did not is large at one point and small at the other. This shows that the concrete stress does not depend solely on either the steel percentage or the magnitude of wheel load. The final concrete stress is primarily controlled by the final state of stress in the slab and the crack spacing to which the pavement eventually stabilizes. If, for instance, before any external load is applied, the internal forces caused by drying shrinkage and temperature decrease have already created enough tension in the slab for the concrete to be on the point of breaking, the addition of an external load will result in an even larger tensile stress in the concrete and cause new cracks to form. On the other hand, as new cracks develop, the crack spacing will be less than before, which will relieve some of the internal tensile stress present when the crack spacing was larger. The final concrete stress, therefore, may actually be the same as before any external load was applied.

The fixed and variable input parameters for the D-series are given below.

Fixed Parameter	Value
Steel property	
P, %	0.7
Diameter, cm	1.25
Yield stress, MPa	41.3
Modulus, GPa	20.0
Coefficient of thermal expansion, (μm/m)/°C	9.0
Concrete property	
Coefficient of thermal expansion, (μm/m)/°C	9.0
Shrinkage coefficient, %	0.04
Unit mass, kN/m³	13.6
Compression strength, MPa	4.1
Temperature data, °C	
Curing	21
Daily min	
1-10	18
11-16	18
17-28	13
Min	-1
Cold time, d	90
Friction	
Pressure, kPa	6.9
Movement, cm	-0.25
External load	
Wheel load, kN	40
Time applied, d	28

Variable Parameter	Problem 1	2	3	4
Concrete property				
D, cm	15.2	20.3	25.4	30.5
External load				
Wheel-load stress, MPa	19.2	12.4	8.43	6.08

The effect of slab thickness on the performance of a continuously reinforced concrete pavement under a 40-kN (9000-lbf) wheel load is plotted in Figure 14. Because a greater slab thickness is accompanied by an increase in the cross-sectional area of the slab, the concrete stress per unit area due to external load decreases as the slab thickness increases. For the external loads, the increase in slab thickness increases the stiffness of the slab, thus reducing the

Figure 10. C-series: final crack spacing versus percentage of steel.

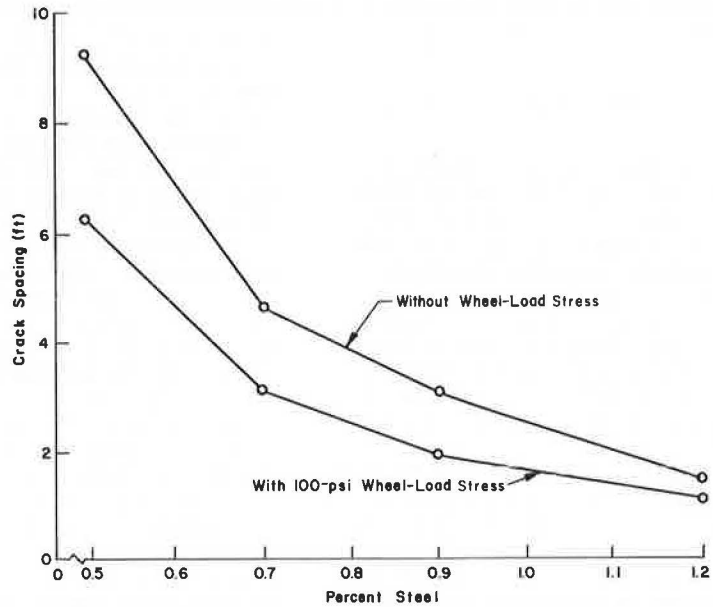

bending stress in the concrete. Consequently, to achieve equilibrium, the net reduction of concrete stress permits the crack spacing to be kept greater for thicker slabs. The increase in crack spacing causes both the steel stress and the crack width to increase.

The fixed and variable input parameters of the E-series are given below and are shown in Figure 15; note that cracks begin to develop immediately after a 1.38-MPa (200 000-lbf/in^2) external load is applied.

Fixed Parameter	Value
Steel property	
P, %	1.0
Diameter, cm	1.25
Yield stress, MPa	41.3
Modulus, GPa	20.0
Coefficient of thermal expansion, (μm/m)/°C	9.0
Concrete property	
D, cm	25.4
Coefficient of thermal expansion, (μm/m)/°C	9.0
Shrinkage coefficient, %	0.04
Unit mass, kN/m^3	13.6
Compression strength, MPa	4.1
Temperature data, °C	
Curing	24
Daily min	
1-10	18
11-16	18
17-28	10
Min	4.5
Cold time, d	90
Friction	
Pressure, kPa	6.9
Movement, cm	-0.25
External load	
Wheel-load stress, MPa	13.8

	Problem		
Variable Parameter	1	2	3
External load			
Time applied, d	7	15	28

The final crack spacings, however, are not affected by the time of load application.

RESULTS

A series of problems were solved by using the CRCP-1 computer program to test the combined effects of wheel-load stress and internal stress on a continuously reinforced concrete pavement. Either the wheel load forces are input and the stresses solved by using Westergaard's equation within the program or the wheel-load stress is solved externally and input directly into the program.

The results show that

1. An increase in wheel-load stress will reduce crack width, crack spacing, and steel stress;
2. An increase in steel percentage will reduce crack width, crack spacing, and steel stress with or without wheel-load stress.
3. An increase in slab thickness will increase crack width, crack spacing, and steel stress; and
4. Cracks developed earlier when wheel loads were applied earlier.

CONCLUSIONS

The following conclusions are made:

The forces acting on the continuously reinforced concrete pavement can be modeled more realistically by using the CRCP-1 computer program that includes both wheel-load stress and environmental stress. The inclusion of wheel load helps to gain greater insight into the real behavior of a continuously reinforced concrete pavement. Warping effect and the fatigue in the slab under repetitive loadings, however, are not considered.

From the limited number of test problems, it was found that the addition of a wheel load on a continuously reinforced concrete pavement has the same effect as increasing the steel percentage in the pavement; both force more cracks to develop. Variation in crack spacing changes the magnitudes of other variables in the pavement, such as steel stress and crack width; lower crack spacing results in lower steel stress and lower crack width. A decrease in slab thickness, on the other hand, has an adverse effect on the behavior

of a continuously reinforced concrete pavement. Increasing the slab thickness can prevent excessive cracking. For the design of a continuously reinforced concrete pavement, it is important to properly correlate the steel percentage and the slab thickness. The final crack spacing should be adjusted to keep the cracks at an optimum width.

ACKNOWLEDGMENTS

This investigation was conducted at the Center for Highway Research, University of Texas, Austin. We wish to thank the sponsors, the Texas State Department of Highways and Public Transportation and the U.S. Department of Transportation, Federal Highway Ad-

Figure 11. C-series: final crack width versus percentage of steel.

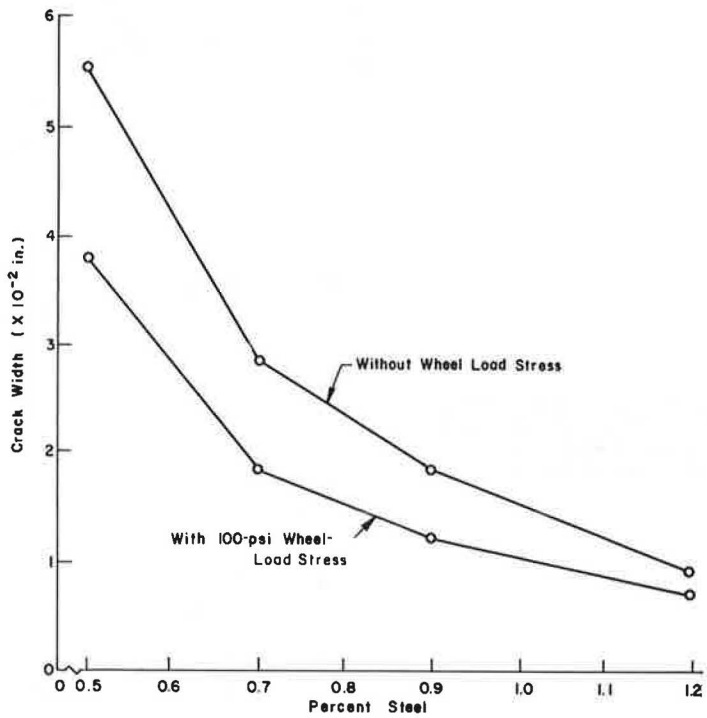

Figure 12. C-series: final steel stress versus percentage of steel.

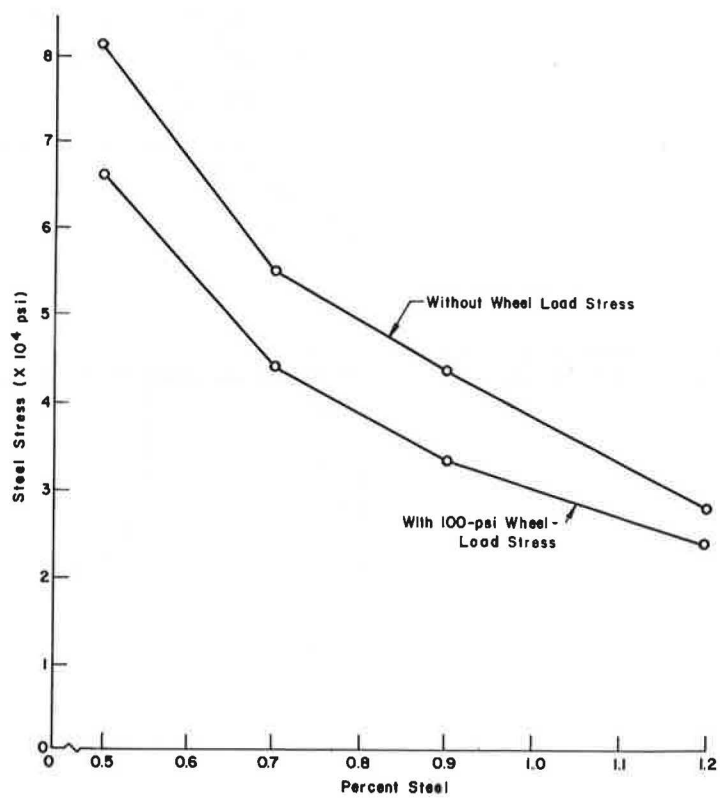

ministration. The contents of this report reflect our views. We are responsible for the facts and the accuracy of the data presented herein. The contents do not necessarily reflect the official views or policies of the Federal Highway Administration. This report does not constitute a standard, specification, or regulation.

REFERENCES

1. B. F. McCullough, A. Abou-Ayyash, W. R. Hudson, and J. P. Randall. Design of Continuously Reinforced Concrete Pavements for Highways. NCHRP, Rept. 1-15, Center for Highway

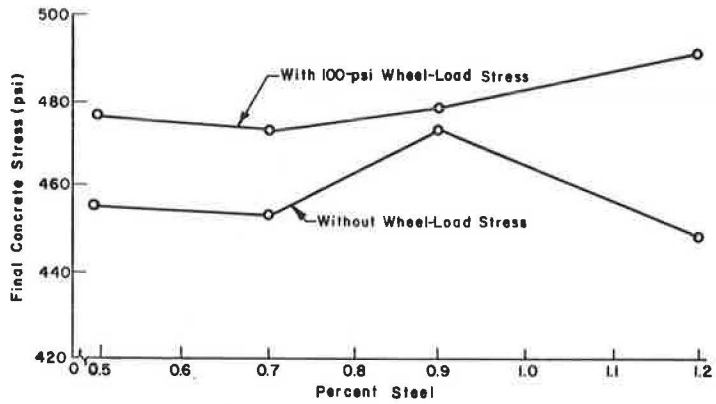

Figure 13. C-series: final concrete stress versus percentage of steel.

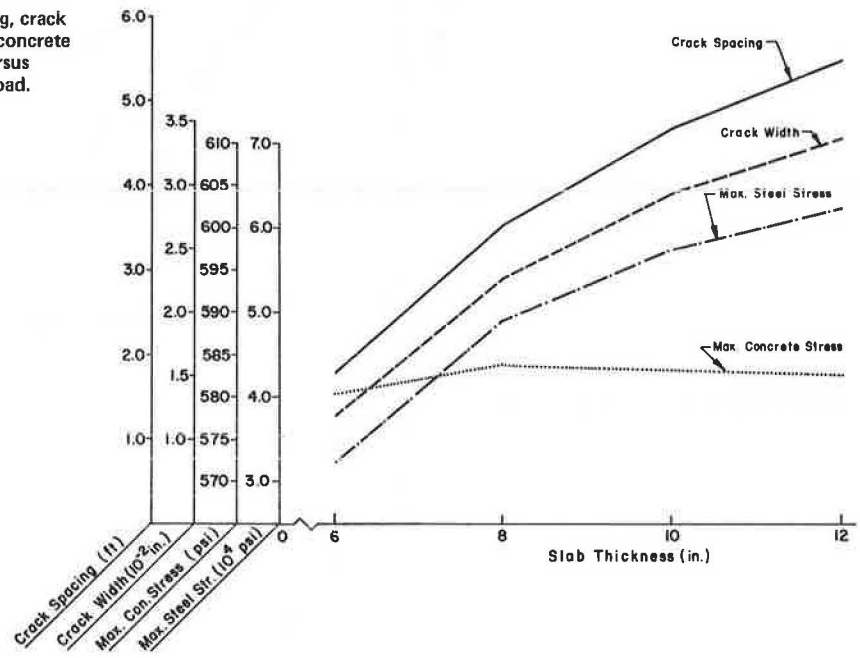

Figure 14. D-series: crack spacing, crack width, steel stress, and maximum concrete stress at end of analysis period versus thickness of slab under external load.

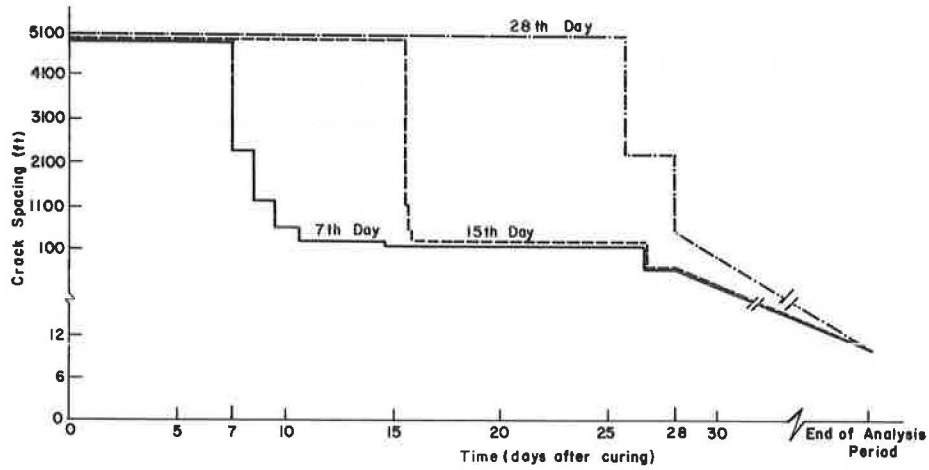

Figure 15. E-series: crack spacing versus time of external load application.

Research, Univ. of Texas, Austin, Aug. 1975.
2. H. M. Westergaard. Computation of Stresses in Concrete Roads. Proc., HRB, Vol. 5, Pt. 1, 1925, pp. 90-112.
3. A. Nadai. Die Biegungsbeanspruchung Von Platten Durch Eingelkrafte. Schweizerische Bauzeitung, Vol. 76, 1970, p. 257; Die Elastischen Pladen, Berlin, 1925, p. 308.
4. R. W. Hudson and H. Matlock. Discontinuous Orthotropic Plates and Pavement Slabs. Center for Highway Research, Univ. of Texas, Austin, Res. Rept. 56-6, May 1966.
5. J. J. Panak and H. Matlock. A Discrete-Element Method of Analysis for Orthogonal Slab and Grid Bridge-Floor Systems. Center for Highway Research, Univ. of Texas, Austin, Res. Rept. 56-25, May 1972.
6. S. Timoshenko and S. Woinowshy-Grieger. Theory of Plates and Shells. McGraw-Hill, New York, 2nd Ed., 1959.
7. F. Endres and H. Matlock. An Algebraic Equation Solution Process Formulated in Anticipation of Bonded Linear Equations. Center for Highway Research, Univ. of Texas, Austin, Res. Rept. 56-19, Jan. 1971.
8. L. D. Childs, B. E. Colley, and J. W. Kapernick. Tests to Evaluate Concrete Pavement Subbases. Journal of the Highway Engineering Division, Proc., ASCE, Vol. 83, No. HW3, July 1957, paper 1297.
9. L. D. Childs and J. W. Kapernick. Tests of Concrete Pavement on Gravel Subbases. Journal of the Highway Engineering Division, Proc., ASCE, Vol. 84, No. HW3, Oct. 1958, paper 1800.
10. A. Abou-Ayyash and R. Hudson. Analysis of Bonding Stiffness Variation at Cracks in Continuous Pavements. Center for Highway Research, Univ. of Texas, Austin, Res. Rept. 56-22, April 1972.

Publication of this paper sponsored by Committee on Rigid Pavement Design.

Procedure for Predicting Occurrence and Spacing of Thermal-Susceptibility Cracking in Flexible Pavements

Samuel H. Carpenter, University of Illinois, Urbana-Champaign
Robert L. Lytton, Texas A&M University

The inability of previous models to accurately predict transverse cracking in pavements in the southwestern United States has led to the laboratory validation of the concept of thermal susceptibility of unstabilized base-course material. Thermal susceptibility is the volumetric contraction of a granular base-course material when it is frozen. This contraction produces cracking in the base course that is highly dependent on the environment in the general area. This paper presents the results of a study that attempted to quantify this mechanism and to predict crack spacings and the rate of crack appearance. The procedure used involves the combination of linear viscoelasticity and linear viscoelastic fracture mechanics. Crack spacings in the base course are calculated by using the results of a finite-element study of the frozen properties of the base course. The effect of these cracks (i.e., the rate at which they propagate reflection cracks through the asphalt surface layer) is determined by using a fracture mechanics approach. Intensity factors are calculated for the viscoelastic thermal stress in the asphalt caused by a temperature cycle and for the stress caused by the deformation of a crack in the base course caused by a freeze. The integration of these distributions in the Paris equation for crack growth gives the number of cycles to failure. These calculations were assembled into a computer model that uses daily climatic data and appropriate material properties to calculate the damage caused by daily temperature cycles. The behavior of asphalt and of sulfur asphalt are contrasted when placed over several base-course materials in two different environments, Abilene and Amarillo, Texas, to illustrate the effects of material-property variation and environmental influence. This model represents an initial theoretical approach to the problem of combining the effects on flexible pavements of environment and traffic to more accurately predict performance. Implications concerning reflection cracking can be drawn directly from the analysis of the effect of thermal susceptibility of the base course on the rate of reflection crack appearance.

To the driving public, cracked pavements are merely uncomfortable and, at worst, may become an irritation. To the engineer, however, the presence of cracking indicates that severe problems are present that will be accelerated by the presence of the cracks. Loss of load-transfer ability, weakening of subgrade stability, debonding, and accelerated rutting are common results seen after cracking is first noticed.

Throughout the southwestern United States, the most common form of cracking that is first visible is typically the transverse crack. This form of deterioration has, in the past, been associated primarily with low temperatures and, as a result, most of the research has concentrated on the fracture susceptibility of asphalt concrete under extremely low temperatures (1, 2, 3), which has not been very accurate for the Southwest. Subsequent studies have incorporated the concept of thermal fatigue and have increased the accuracy for predictions in the Southwest (1).

Recent studies of environmental effects on pavements in the west Texas area, however, have conclusively shown that there is a previously unconsidered environmental mechanism acting (4, 5, 6). This mechanism, thermal susceptibility, involves the contraction of an unstabilized granular base course when its temperature drops below freezing. The magnitude of this contraction is related to the environment (7) and material